Laser-driven magneto-inertial fusion with magnetized cylindrical target

Laser-driven magneto-inertial fusion with magnetized cylindrical target

V V Kuzenov[1,2], V V Shumaev[1] and A O Dobrynina[1]

[1] Department of Thermal Physics, Bauman Moscow State Technical University, 2 Baumanskaya Street 5, 1, Moscow 105005, Russia
[2] Dukhov All-Russian Research Institute of Automatics (State Corporation «ROSATOM» company), Suschevskaya Street 22, Moscow 127055, Russia

E-mail: svryzhkov@bmstu.ru, vik.kuzenov@gmail.com

Abstract. Laser-driven magneto-inertial fusion assumed plasma and magnetic flux compression by quasisymmetric laser-driven implosion of magnetized target. We develop a 1D radiation magnetohydrodynamic code and a formulation for the one-fluid two-temperature equations for simulating compressible non-equilibrium magnetized target plasma. Laser system with pulse radiation with 10 ns duration is considered for numerical experiments. A numerical study of a scheme of magnetized laser-driven implosion in the external magnetic field is carried out.

1. Introduction

A magneto-inertial (MIF) version of the thermonuclear scheme with a laser driver [1-9] is considered in the work. This scheme is based on the general idea of adiabatic acceleration (compression) by a laser pulse of a target consisting of a pre-formed low-temperature plasma and a "frozen" magnetic field in the plasma [10-15]. The important thing is the impulse nature of MIF. In this case, not all possible plasma instabilities can develop, but only those that are rapidly growing with time. To study the physical and technical properties of the MIF scheme, a one-dimensional axisymmetric computational model is used in the active zone of a pulsed thermonuclear reactor (MIF).

2. Mathematical model

Here we present a one-dimensional mathematical model of compression and combustion processes of thermonuclear targets of MIF for an axisymmetric coordinate system. This model is based on one-dimensional single-fluid, two-temperature equations of magneto-radiation gas dynamics. The mathematical model did not take into account the process of generation of fast electrons. Because when the laser radiation interacts with the MIF plasma, whose density is less than the critical one, there is no resonance absorption of the radiation, which is the cause of the most efficient mechanism for the generation of fast electrons at laser radiation intensities. Electromagnetic processes occurring in a thermonuclear target and the plasma region surrounding it are described by a system of Maxwell and Ohm equations with finite plasma conductivity.

$$\frac{\partial \rho}{\partial t} + Div\left(\rho u\right) = F_{\rho}\,,\ F_{\rho} = -\rho u \frac{\left(v-1\right)}{r}\,, \tag{1}$$

$$\frac{\partial(\rho u)}{\partial t} + Div\left(\rho u^2 + P\right) = F_{\rho u} + f_r,\ F_{\rho u} = -\rho u^2 \frac{(v-1)}{r},\ f_r = \frac{1}{c}\left[\vec{j} \times \vec{H}\right]_r,)$$

$$\frac{\partial(\rho E)}{\partial t} + Div\left(\rho E u + P u + q_\Sigma\right) = F_E + q_r + Q^e_{Fus},\ q_r = j_r E_r,\ q_\Sigma = q_e + q_i + q_{лаз},$$

$$F_E = -\left(\rho E u + P u\right)\frac{(v-1)}{r},\ P = P_e + P_i,\ Div(\ ) = \frac{1}{J}\frac{\partial(J\ )}{\partial \xi},\ J = r^{(v-1)},$$

where t is the time, r is the radial coordinate, u is the velocity along r, $P = P(\rho, \varepsilon)$ is the static pressure, ε is the specific internal plasma energy, $E = \left(\varepsilon + u^2/2\right)$ is the total gas flow energy, $\vec{F} = \left(F_\rho, F_{\rho u}, F_E\right)$ is the source vector in an orthogonal coordinate system, $F_\rho, F_{\rho u}, F_E$ are the density of mass flow, momentum, energy, referred to the radial coordinate r, q, q_v are the full and spectral radiation flux, T_e, T_i are the electron and ion temperature $\left(T = T_e = T_i\right)$, f_r is the electromagnetic force, q_r is the energy flow from the electromagnetic field, $q_e = -\lambda_e grad T_e$, $q_i = -\lambda_i grad T_i$, q_{las} is the laser flux, λ_e, λ_i are the electron and ion thermal conductivity coefficients, j_r is the current density, $\vec{H}(r)$ is the magnetic induction vector, P_e, P_i are the electron and ion pressure respectively, $v = (1, 2)$ are indexes, corresponding to plane and axial symmetry.

The transfer of broadband radiation is considered within the framework of the multigroup diffusion approximation:

$$\frac{1}{r^n}\frac{d\left(r^n q_v\right)}{dr} + \chi_v c U_v = \chi_v 4\sigma T^4,\ \frac{c}{3}\frac{dU_v}{dr} + \chi_v q_v = 0, \tag{2}$$

where q_v, U_v are the spectral flux (radial flux in the direction of the axis *r*) and bulk density (radiation power density) of broadband radiation, c is the speed of light in vacuum, v is the frequency band number, χ_v is the spectral absorption coefficient, n = 0 corresponds to flat and n = 1 to endless cylinder.

The equation of magnetic induction takes into account the continuity equation for density and the conservation law:

$$\frac{\partial(B_z/\rho)}{\partial t} + \frac{1}{\mu J}\frac{\partial J(\mathrm{v}B_z/\rho)}{\partial r} = \frac{c^2}{4\pi\mu\rho Jr}\frac{\partial}{\partial r}\left(\frac{Jr}{\sigma}\frac{\partial B_z}{\partial r}\right). \tag{3}$$

The parameters of the laser radiation along the axis are based on the solution of the laser radiation transfer equation:

$$\frac{dq_{laz}}{dz} - \chi_\omega q_{laz} = 0, \tag{4}$$

where τ is the half-width of the laser pulse at half-height. The absorption coefficient of laser radiation is determined using the mechanism of continual absorption inverse to the bremsstrahlung mechanism of electrons under conditions of local thermodynamic equilibrium (LTE):

$$\chi_\omega = \begin{cases} \dfrac{4{,}97 g Z_i^2 n_i^\Sigma n_e^\Sigma}{n_c^2 \lambda^2 \left(kT_e\right)^{3/2}} \dfrac{1}{\sqrt{1 - n_e/n_c}}, & n_e < n_c \\ \infty, & n_e \geq n_c \end{cases},$$

where λ is the laser radiation wavelength (mcm), n_e, n_i are the electron and ion densities correspondingly (cm^{-3}), kT_e is the electron temperature (keV), g is the Gaunt factor, $n_c = 10^{21} \times \lambda^{-2}$ is the critical electron density (cm^{-3}) [11-14].

The calculation of the thermodynamic and optical parameters of the working media included in this system of equations was carried out within the framework of the LTE approximation. A MATTINA (MAgnetized inerTial Target in Numerical Analysis) for the nonstationary radiation magneto-gasdynamics models for describing the plasmadynamic processes in different MIF schemes are developed.

The detailed mathematical model is presented in Ref. 16-19.

3. Calculation results

Modeling calculations based on the proposed numerical method for solving the system of gas dynamics equations are performed. Laser system with pulse radiation with 10 ns duration is considered. Numerical simulation of the magnetized target compression is done for $q_{laz} \leq 10^{14}$ W/cm^2. Initial values of the intensity of a seed magnetic field in the rarefied medium reach a fraction of Tesla. A computational domain and target of magneto-inertial fusion consist of the central part and one coaxial layer. They have a cylindrical shape with the following range of values of initial parameters of target and medium. The central part of the target (inner radius R = 0.05 cm) is filled with D-T mixture with density $\rho = 5 \times 10^{-2}$ g/cm^3 and temperature of T = 297 K. It was surrounded by the coaxial layer (outer radius $R_c = 0.1$ = 0.1 cm) consisting of metal (Aluminum) with density ρ = 2.7 g/cm^3 and temperature of T = 297 K. The computational domain has outer radius r = 0.2 cm. Thermodynamic parameters of external rarefied medium (Argon) are defined: T = 297 K, $\rho = 1.29 \times 10^{-3}$ g/cm^3. Theoretical results for the case of double-layer target for laser-driven magneto-inertial fusion are presented below. The dynamics of the magnetized plasma expansion into an ambient gas is considered. The key parameters of the laser-target system are calculated. Calculations carried out for the Nd laser radiation for forming rectangular shape (impulse duration t_{las} = 10 ns). The radiant flux value is $q_{laz} = 10^{14}$ W/cm^2. A thin metallic cylindrical shell material is Al. The target radius is 0.1 cm.

Next, we consider the results of numerical simulation of the effect of an intense flux (laser radiation energy density of 10^{15} W/cm^2) of laser radiation on a target, which is affected by an external magnetic field of the order of several T. The computational domain, the geometry of the target, the range of values of the initial parameters of the target are similar to the above case. The values of the initial environmental parameters are the following: the thermodynamic parameters of the external rarefied environment (consists of Ar) are given by the values: T = 297 K, ρ = 2.7·10-3 g/cm^3. The spectral flux and bulk density of the broadband radiation, as well as the laser radiation flux are zero for the initial moment of time.

Spatial distributions corresponding to the initial stage of exposure to laser radiation on the target are presented on figures 1 and 2. Here, at high temperatures (T > 105 K), the nonlinear mechanism of heat energy transfer by radiant heat conduction manifests itself [20-21]. In this case, the transfer of energy in space occurs due to broadband radiation. At the same time, the speed of such a transfer can be substantially greater than the speed of sound and the walls of the target are practically immobile.

However, from the spatial distributions shown in figure 1 it follows that there is a macroscopic motion near the outer boundary of the target (the region of intense absorption of laser radiation); this motion due to the discontinuous nature of the pressure, velocity and density distributions (and the Rankine–Hugoniot conditions at breaks) corresponds to two shock waves of different intensity moving with speeds lower than the “heat waves” speeds. These shock waves (speed of movement behind the right shock wave +250 km / s, and behind the left -30 km/s) are formed in the environment and on the outer (cm) target wall by the movement of the target material vapor under the action of laser radiation. Note also that by this time point there is a relatively weak change in magnetic pressure (figure 2).

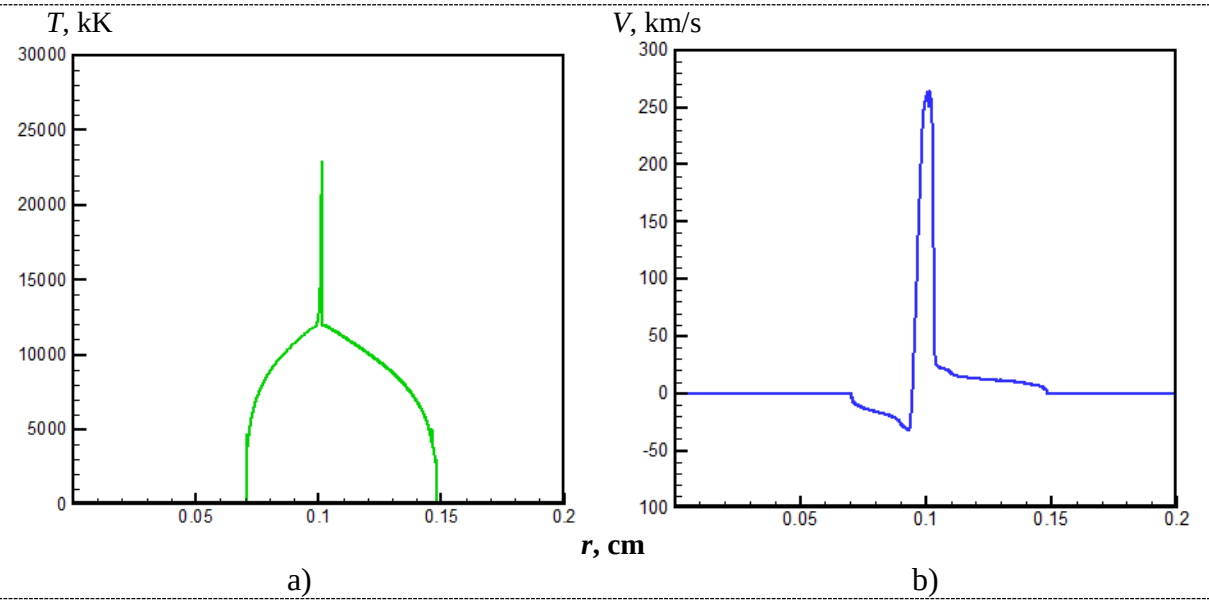

Figure1. Spatial distribution of the plasma temperature (a) and velocity (b) for the laser energy flux density 10^{15} W/cm^2 at time 0.18 ns.

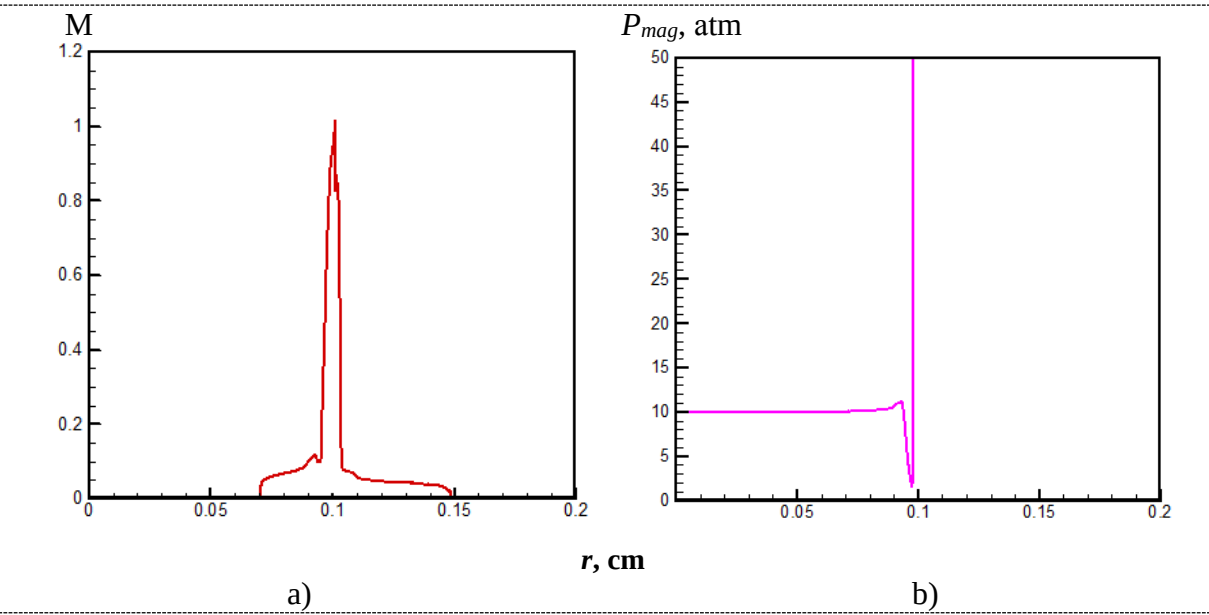

Figure 2. Spatial distribution of the Mach number a) and magnetic pressure b) at time t = 0.18 ns.

Further figures 3, 4 present the spatial distributions for exposure to laser radiation, corresponding to the stage of the "thermal wave" reaching the geometric axis of the target. In this case, the maximum of temperature and pressure is located on the geometrical axis of the target and reaches the values $T = 18 \cdot 10^6$ K and $P = 4.5 \cdot 10^7$ atm. The front of the “heat wave” at the considered time point t = 0.48 ns (figure 3) is r_f = 0.23 cm. In this case, the “heat wave” in front of itself formed a compression wave (figure 4) with the coordinate of the wave front r_{SW} = 0.24 cm. In addition to this shock wave, in the

$0 \le r \le 0.1$ cm region occupied by the flow of the target plasma, several more shock wave structures are present.

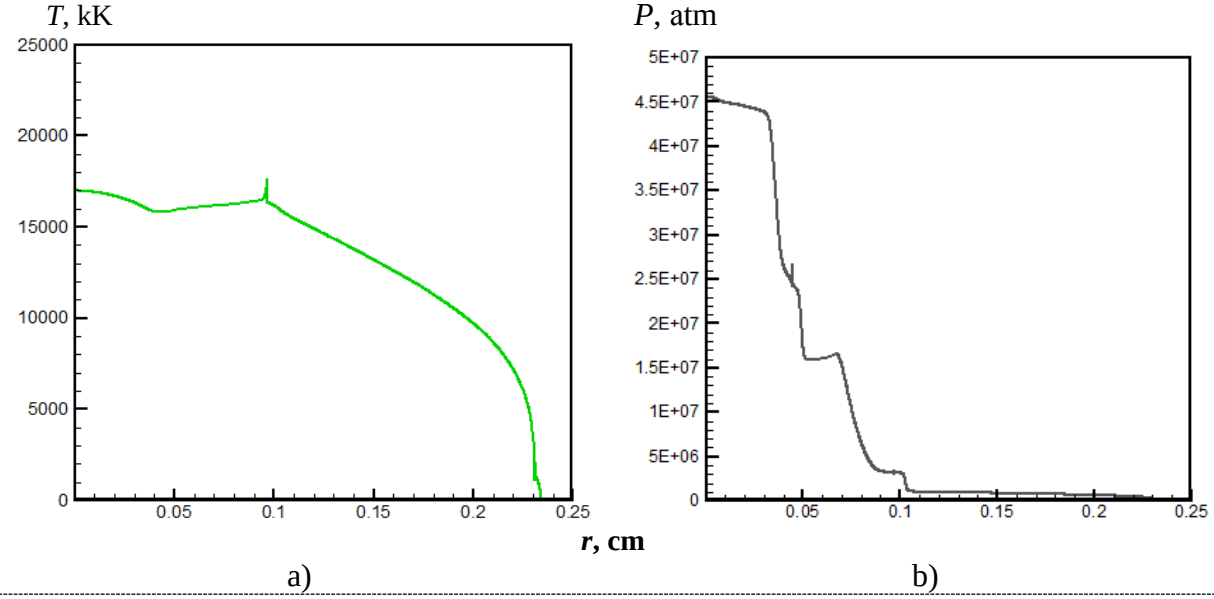

Figure 3. The distribution of the plasma temperature a) and pressure b) at time 0.48 ns.

The first structure (figure 4) is located in the interval of coordinates cm and is the development of a system of shock waves (the speed of motion behind the right shock wave is +350 km/s, and behind the left is 40 km/s) created by the movement of vapor from the target material of the outer part of the target under the action of laser radiation. The second structure with an interval of centimeters cm is also formed by the movement of vapors (the speed of movement behind the right shock wave is +100 km/s, and behind the left -20 km/s), but on the inner boundary of the target.

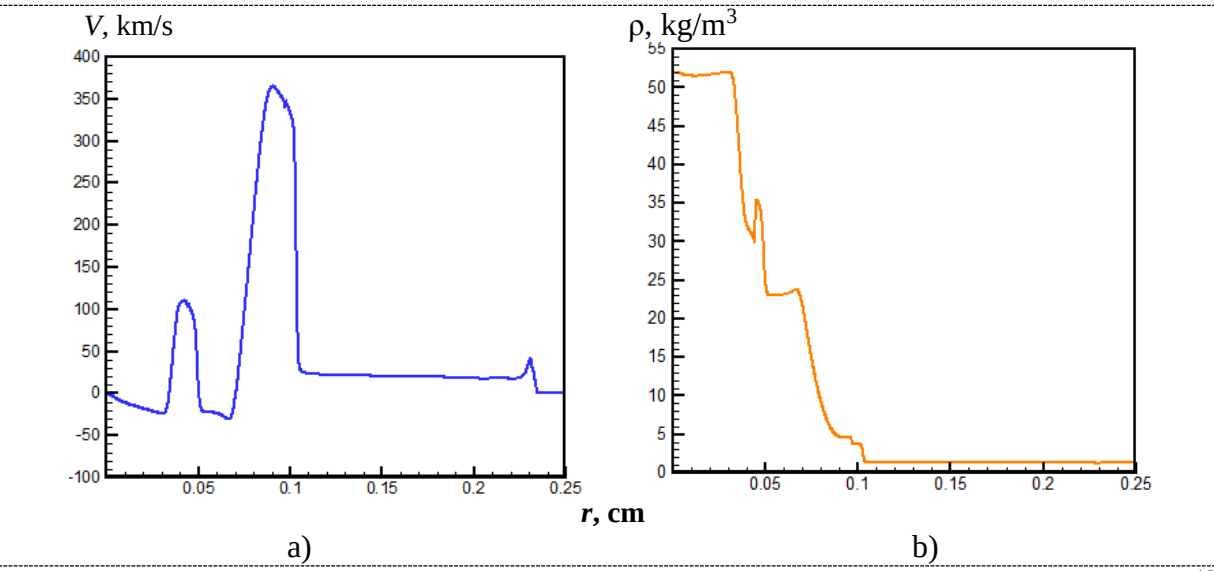

Figure 4. Spatial distribution of the velocity a) and density b) for the laser energy flux density 10^{15} W/cm^2 at time t = 0.48 ns.

4. Conclusion

We have developed a model for laser-driven magneto-inertial fusion-laser-driven target implosion in an externally applied magnetic field. The main plasma parameters (pressure P, temperature T, velocity V and density ρ), magnetic field characteristics (magnetic pressure P_{mag}) and laser radiation parameters (energy W_{las} and combined flux of the self-radiation of plasma W_s) along the radial coordinate are calculated. Numerical modeling of the laser target compression process showed the following. The central part of a target is optically transparent for both laser and own broadband plasma radiation during compression. However at the same time heat flow density on the first wall of the reactor chamber at a certain moment of time can reach 10^8 W/cm^2. The magnetic pressure P_{mag} during compression of a target changes in time and is comparable to the static pressure P, reaching values 10^6 atm. The maximum values of plasma pressure and temperature of a magneto-inertial fusion are observed after reflection of a shock wave from a geometrical axis of symmetry at t = 5 ns.

This research has been partially supported by the Russian Ministry of Science and Higher Education (No. 13.5240.2017/8.9), BMSTU Target Program for 2018-2020, performed at “Beam-M”.

References

[1] Velikhov E P, Vedenov A A, Bogdanets A D, Golubev V S, Kasharskii E G, Kiselev A A, Rutberg F G and Chernukha V V 1973 *Sov. J. Tech. Phys.* 18 274–283
[2] Gasilov V A, Zakharov S V and Smirnov V P 1991 *JETP Lett.* 53 85–88
[3] Ryzhkov S V, Khvesyuk V I and Ivanov A A 2003 *Fusion Sci. Technol.* 43(1T) 304-308
[4] Kostyukov I Yu and Ryzhkov S V 2010 *Plasma Phys. Rep.* 37 1092–1098
[5] Chirkov A Yu, Ryzhkov S V, Bagryansky P A, Anikeev A V 2011 *Fusion Science and Technology* 59(1T) 39-42
[6] Ryzhkov S V 2015 *Sustain. Cities Soc.* 14 313–315
[7] Aleksandrov V V, Bolkhovitinov E A, Volkov G S, Grabovski E V, Gritsuk A N, Medovshchikov S F, Oleinik G M, Rupasov A A and Frolov I N 2016 *Plasma Phys. Rep*. 42 1091–1100
[8] Honrubia J J, Murakami M, Mima K, Johzaki T, et al 2016 *J. Phys.: Conf. Ser*. 688 012033
[9] Crandall D H 2016 *J. Phys.: Conf. Ser.* 717 012001
[10] Thio Y C F 2008 *J. Phys.: Conf. Ser.* 112 042084
[11] Kuzenov V V, Ryzhkov S V, Shumaev V V 2015 *Probl. At. Sci. Technol.* No. 4 (98) 53-56
[12] Ryzhkov S V, Chirkov A Y and Ivanov A A 2013 *Fusion Sci. Technol.* 63 135–138
[13] Kuzenov V V, Ryzhkov S V, Shumaev V V 2015 *Probl. At. Sci. Technol.* No. 1 (95) 97-99
[14] Kuzenov V V and Ryzhkov S V 2016 *Bull. Russ. Acad. Sci.: Phys.* 80 598–602
[15] Nagatomo H, Johzaki T, Asahina T and project group F 2016 *J. Phys.: Conf. Ser*. 717 012041
[16] Kuzenov V V, Ryzhkov S V and Frolko P A 2017 *J. Phys.: Conf. Ser*. 830 012049
[17] Kuzenov V V and Ryzhkov S V 2014 *Applied Phys.* 3 26-30
[18] Kuzenov V V and Ryzhkov S V 2018 *Math. Models Comput. Simul.* 10 255-264
[19] Kuzenov V V and Ryzhkov S V 2017 *J. Phys.: Conf. Ser*. 830 012124
[20] Zarubin V S, Kuvyrkin G N and Savelyeva I Y 2015 *High Temperature* 53, 234–239
[21] Dimitrienko Y, Koryakov M, and Zakharov 2017 Lecture Notes in Computer Science (including subseries Lecture Notes in Artificial Intelligence and Lecture Notes in Bioinformatics) 10187, 294-301